Systems/Circuits

Sexually Dimorphic Neurosteroid Synthesis Regulates Neuronal Activity in the Murine Brain

Philipp Wartenberg,[1] Imre Farkas,[2] Veronika Csillag,[3,4] William H. Colledge,[5] Erik Hrabovszky,[2] and Ulrich Boehm[1]

[1]Experimental Pharmacology, Center for Molecular Signaling, Saarland University School of Medicine, Homburg, 66421, Germany, [2]Laboratory of Reproductive Neurobiology, Institute of Experimental Medicine, Budapest, 1083, Hungary, [3]Laboratory of Endocrine Neurobiology Institute of Experimental Medicine, Budapest, 1083, Hungary, [4]Tamás Roska Doctoral School Péter, Pázmány Catholic University, Budapest, 1083, Hungary, and [5]Department of Physiology, Development and Neuroscience, University of Cambridge, Cambridge, CB2 1TN, United Kingdom

Sex steroid hormones act on hypothalamic kisspeptin neurons to regulate reproductive neural circuits in the brain. Kisspeptin neurons start to express estrogen receptors *in utero*, suggesting steroid hormone action on these cells early during development. Whether neurosteroids are locally produced in the embryonic brain and impinge onto kisspeptin/reproductive neural circuitry is not known. To address this question, we analyzed aromatase expression, a key enzyme in estrogen synthesis, in male and female mouse embryos. We identified an aromatase neuronal network comprising ~6000 neurons in the hypothalamus and amygdala. By birth, this network has become sexually dimorphic in a cluster of aromatase neurons in the arcuate nucleus adjacent to kisspeptin neurons. We demonstrate that male arcuate aromatase neurons convert testosterone to estrogen to regulate kisspeptin neuron activity. We provide spatiotemporal information on aromatase neuronal network development and highlight a novel mechanism whereby aromatase neurons regulate the activity of distinct neuronal populations expressing estrogen receptors.

Key words: **aromatase; estrogen receptor; hypothalamus; *in utero*; kisspeptin; paracrine**

Significance Statement

Sex steroid hormones, such as estradiol, are important regulators of neural circuits controlling reproductive physiology in the brain. Embryonic kisspeptin neurons in the hypothalamus express steroid hormone receptors, suggesting hormone action on these cells *in utero*. Whether neurosteroids are locally produced in the brain and impinge onto reproductive neural circuitry is insufficiently understood. To address this question, we analyzed aromatase expression, a key enzyme in estradiol synthesis, in mouse embryos and identified a network comprising ~6000 neurons in the brain. By birth, this network has become sexually dimorphic in a cluster of aromatase neurons in the arcuate nucleus adjacent to kisspeptin neurons. We demonstrate that male aromatase neurons convert testosterone to estradiol to regulate kisspeptin neuron activity.

Introduction

Sex steroid hormones are important regulators of the neural circuits controlling reproductive physiology and behavior in the brain (McCarthy, 2008; Micevych and Meisel, 2017; Balthazart, 2020; Ventura-Aquino and Paredes, 2020). Within this neuronal network, sex steroid signals are detected by kisspeptin neurons in the hypothalamus and then relayed to gonadotropin releasing hormone (GnRH) neurons (Pielecka-Fortuna et al., 2008; Lehman et al., 2010; Mayer et al., 2010; Dubois et al., 2015, 2016; Yip et al., 2015; Wang et al., 2018). GnRH is released from axon terminals in the median eminence at the base of the brain and then acts on gonadotrope cells in the anterior pituitary gland to regulate gonadal function (Glanowska et al., 2012; Candlish et al., 2018). Synaptic communication between kisspeptin and GnRH neurons is established during embryonic development of the murine brain (Kumar et al., 2014, 2015). Embryonic kisspeptin neurons start to express estrogen receptor α (ERα) in both males and females and androgen receptor (AR) in males, suggesting that the kisspeptin/GnRH neural circuits become steroid-hormone-sensitive *in utero* and raising the possibility that

Received Apr. 22, 2021; revised Aug. 12, 2021; accepted Sep. 10, 2021.

Author contributions: P.W., I.F., and V.C. performed research; P.W., I.F., V.C., and E.H. analyzed data; I.F., W.H.C., and E.H. edited the paper; P.W., E.H., and U.B. designed research; W.H.C. contributed unpublished reagents/analytical tools; P.W. and U.B. wrote the first draft of the paper; U.B. wrote the paper.

This work was supported by Deutsche Forschungsgemeinschaft SFB 894 and SFB/TR152 to U.B.; National Science Foundation of Hungary K128317 and K138137; and Hungarian Brain Research Program 2017-1.2.1-NKP-2017-00002 to E.H. We thank Nirao Shah (Stanford University) for providing the Aromatase-IRES-Cre mice.

The authors declare no competing financial interests.

Correspondence should be addressed to Ulrich Boehm at ulrich.boehm@uks.eu or Erik Hrabovszky at hrabovszky.erik@koki.hu.

https://doi.org/10.1523/JNEUROSCI.0885-21.2021

steroid hormones may act on these cells early during development.

Sex steroids are not only gonadal in source but can also be produced locally in the brain (Kenealy et al., 2013, 2017). Aromatase is encoded by the *Cyp19a1* gene and converts androgen into estrogen (Santen et al., 2009). Aromatase expression has been detected in the brain of different species (Balthazart et al., 1991; Wagner and Morrell, 1997; Sasano et al., 1998; Wacker et al., 2016). Whether neurosteroids are locally produced in the embryonic mouse brain and impinge onto kisspeptin/GnRH neural circuits is not known. At late embryonic stages and during the first days after birth in rodents, estrogen is needed in males to masculinize the brain (Scordalakes and Rissman, 2004; McCarthy, 2008; Wu et al., 2009). Consistent with this, blocking of estrogen access prevents defeminization of the male brain (Vreeburg et al., 1977). During this critical time period, α-fetoprotein protects the embryos from maternal estrogen synthesized in the placenta (Toran-Allerand, 2005; Bakker et al., 2006; De Mees et al., 2007).

Reliable antibodies against aromatase have been difficult to produce because of the enzyme's localization in the membrane of the endoplasmic reticulum. The detection of aromatase mRNA in the brain has been hampered by low expression levels in this tissue. More recently, reporter mouse strains have provided important insights into aromatase expression in the rodent brain (Wu et al., 2009; Stanic et al., 2014). These studies identified aromatase neurons in distinct regions important for sexual and aggressive behavior and reproduction (Unger et al., 2015) and demonstrated that aromatase expression is sexually dimorphic in adults. Aromatase is already expressed in the brain before puberty and is important for the masculinization of the brain (Wu et al., 2009). While previous studies had provided some experimental evidence for aromatase expression in the embryonic rodent brain (Sanghera et al., 1991; Lephart et al., 1992; Lauber and Lichtensteiger, 1994), the individual neurons and the respective neural circuits expressing aromatase *in utero* have remained elusive.

Capitalizing on reporter mice, we find that aromatase is specifically expressed in distinct neurons in the murine forebrain as early as embryonic day 13.5, developing into an aromatase network comprising ~6000 neurons in the hypothalamus and the amygdala *in utero*. At birth, we identified a cluster of aromatase neurons in the arcuate nucleus immediately adjacent to kisspeptin neurons in the male, but not in the female hypothalamus. We demonstrate that testosterone (T) impinges on the firing activity of kisspeptin neurons, likely mediated by estradiol through endogenous aromatization in the brain.

Materials and Methods

Experimental design. We analyzed aromatase expression *in utero* and after birth capitalizing on the Aromatase-IRES-Cre (*ArIC*) (Unger et al., 2015) knock-in mouse strain crossed with eROSA26-τGFP (*eR26-τGFP*) (Wen et al., 2011) animals, resulting in *ArIC/eR26-τGFP* reporter mice. Expression from the *ROSA26* locus results in τGFP exclusively labeling aromatase-expressing cells and fibers enabling quantification of τGFP-expressing neurons ($n = 3$-5 for males and $n = 3$ or 4 for females). Acute expression of aromatase and other key genes of the estrogen synthesis chain was analyzed by qPCR ($n = 3$ or 4 animals per age and sex). Relation of τGFP cells to ERα-expressing cells was investigated by measuring the distance between τGFP and ERα neurons ($n = 3$ for each sex and age). Whole-cell patch-clamp recordings in kisspeptin neurons were used to investigate the influence of estrogen on kisspeptin neuron firing in 4-7 d old males ($n = 33$ cells) and females ($n = 6$ cells; Extended Data Tables 8-1, 8-2, and 8-3).

Mice. Animal care and experimental procedures were approved by the animal welfare committee of the Saarland University and performed in accordance with their established guidelines. Mice were kept under a standard light/dark cycle (lights on at 7:00 A.M. and off at 7:00 P.M.) with food and water *ad libitum*. To label aromatase-expressing cells, we crossed *ArIC* mice with *eR26-τGFP* animals. In the resulting *ArIC/eR26-τGFP* mice, Cre recombinase is bicistronically expressed under control of the *Cyp19a1* promotor. Cre-mediated recombination results in the removal of a strong transcriptional stop cassette from the *ROSA26* locus and subsequent constitutive expression of τGFP exclusively labeling aromatase expressing cells and fibers. All animals used in this study were heterozygous for the *ArIC* and the *eR26-τGFP* alleles, respectively, and analyzed at the following developmental stages: embryonic day 12.5 (E12.5), E13.5, E16.5, and E18.5 and at postnatal day 0 (P0).

KP-ZsGreen transgenic mice used for whole-cell patch-clamp electrophysiology were generated by breeding *Kiss1-Cre* transgenic mice (Yeo et al., 2016) with the *Gt(ROSA)26Sor_CAG/LSL_ZsGreen1 Tm* indicator strain (The Jackson Laboratory, JAX #007906) at the Medical Gene Technology Unit of the Institute of Experimental Medicine, Budapest, Hungary. Newborn (P4-P7) male and female *KP-ZsGreen* mice heterozygous for the *KP-Cre* allele were housed in light- (12:12 light-dark cycle, lights on at 06:00 h) and temperature-controlled environment (22 ± 2° C), with free access to standard food and water. All animal studies were conducted with permissions from the Animal Welfare Committee of the IEM (Permission #A5769-01) and in accordance with legal requirements of the European Community (Directive 2010/63/EU). Experiments were designed in accord with accepted standards of animal care and all efforts were made to minimize animal suffering.

Tissue preparation. Embryonic tissue was prepared as described previously (Kumar and Boehm, 2014). In brief, pregnant mice were anesthetized and killed, the embryos removed, washed in ice-cold PBS, and immersed in 4% PFA on ice overnight. Whole embryos (E12.5 and E13.5) or embryo heads (E16.5 and E18.5) were then transferred to 30% sucrose and kept at 4°C until they sank. The embryos were frozen in optimal cutting solution (Leica Microsystems), and 14 µm sagittal sections were prepared using a cryostat. Embryo tail biopsies were digested in lysis buffer, genotyped, and used for sex determination by PCR (Agulnik et al., 1997), as described previously (Kumar and Boehm, 2014). At P0, mice were perfused transcardially with 4% PFA under ketamine/xylazine anesthesia. Brains were removed, postfixed in 4% PFA for 2 h on ice, transferred to 30% sucrose at 4°C until they sank, and frozen in tissue freezing medium (Leica Microsystems). Coronal sections (14 µm) were prepared using a cryostat (Leica Microsystems) and stored at −80°C until use.

Immunofluorescence. Sections from *ArIC/eR26-τGFP* mice were incubated in PBS with 10% donkey serum (Jackson ImmunoResearch Laboratories), 3% BSA (Sigma), and 0.3% Triton X-100 for 1 h at 20°C-25°C, followed by incubation with chicken anti-GFP antiserum (1:1000; A10262; Invitrogen), diluted in PBS at 4°C overnight. Sections were then incubated in goat anti-chicken Alexa-488 (1:500; A11039; Invitrogen) in PBS for 2 h at 20°C-25°C. Subsequently, sections were either incubated in primary antisera against ERα (1:1000; 06–935; Millipore), diluted in PBS (overnight at 4°C), or against kisspeptin (1:500, AB9754, Millipore), diluted in PBS (48 h at 4°C), and then treated with anti-rabbit IgG antiserum (1:500; 711-165-152; Jackson ImmunoResearch Laboratories), diluted in PBS, for 2 h at 20°C-25°C. Nuclei were stained with Hoechst solution (1:10,000, Sigma) in PBS for 10 min, and the sections were mounted with Fluoromount-G (Southern Biotechnology). Slides were analyzed on an Axioskop2 microscope equipped with AxioVision software (Carl Zeiss) or an Axio Scan.Z1 with Zen-Blue software (Carl Zeiss).

Quantification of neurons. Neurons were manually counted in every fifth section using the ImageJ Cell Counter plugin. τGFP and kisspeptin

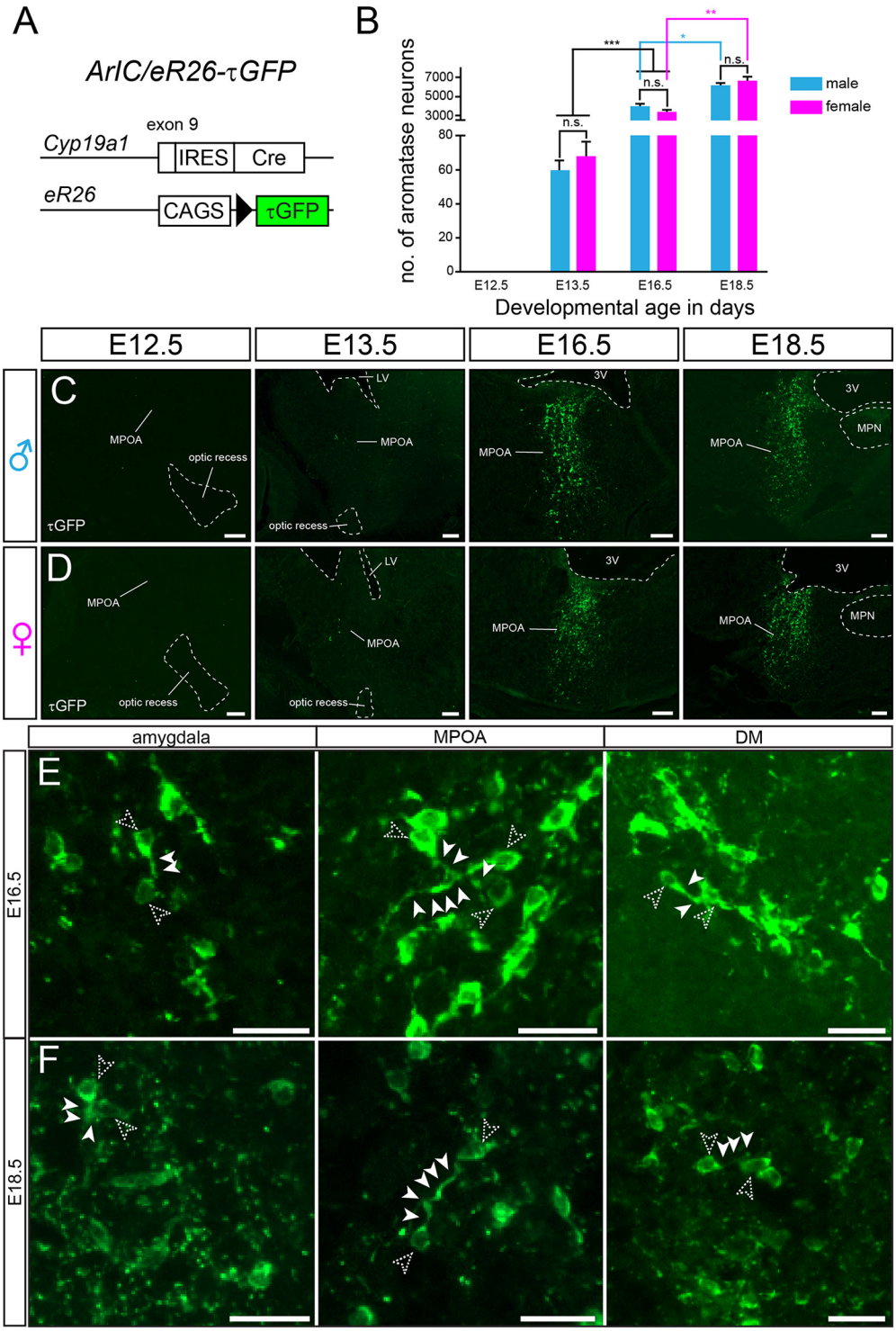

Figure 1. Genetic analysis of aromatase expression in mouse embryos. ***A***, Aromatase and τGFP reporter expression are genetically coupled in *ArIC/eR26-τGFP* mice, providing a fluorescent readout for *Cyp19a1* promotor activity. ***B***, Quantification of aromatase neurons during embryonic development (E13.5 vs E16.5 unpaired Student's *t* tests: $p < 0.0001$; E16.5 male vs E18.5 female unpaired Student's *t* tests: $p = 0.0127$; E16.5 vs E18.5 female unpaired Student's *t* tests: $p = 0.0035$). Detailed cell counts for each nucleus are reported in Extended Data Tables 1-1, 1-2, and 1-3. ***C***, ***D***, Reporter expression in the MPOA at E12,5, E13.5, E16.5, and E18.5. ***E***, ***F***, Numerous contacts between aromatase perikarya (unfilled arrowheads) and fibers (filled arrowheads) as shown in the amygdala, MPOA, and dorsomedial nucleus (DM). Scale bars: ***C***, ***D***, 100 μm; ***E***, ***F***, 25 μm. 3V, third ventricle; LV, lateral ventricle, MPN, median preoptic nucleus, MPOA, medial preoptic area.

neurons were counted based on positively stained cytoplasm, and ERα neurons were counted based on nuclear signal. Counted numbers were multiplied by 2.5 to estimate the total number of neurons per brain (Boehm et al., 2005). Fiber density was qualitatively determined and grouped in four different categories based on intensity.

ERα distance measurements. Distances between τGFP-positive, but ERα-negative neurons and τGFP-negative/ERα-positive cells were calculated with the line tool in the Zen-Blue software (Carl Zeiss). Randomly chosen cells from 3 different animals per age and sex group were included in the calculation.

Quantitative RT-PCR. Total RNA from E12.5, E13.5, E16.5, and E18.5 embryo brains was isolated with the RNeasy Mini Kit (QIAGEN) according to the manufacturer's instructions, and the RNA concentration was measured using a Nanodrop. Total RNA was treated with DNase (TURBO DNA-free kit, Invitrogen) before cDNA was synthesized using the Maxima First Strand kit (Thermo Fisher Scientific) according to the manufacturer's instructions. qRT-PCR reactions with primers against *Cyp11a1*, *Cyp17a1*, *Cyp19a1*, and *β-actin* were performed using the SensiFAST SYBR No-ROX kit (Bioline). Controls without template and without reverse transcriptase, respectively, were included.

Brain slice preparation. Neonatal male and female *KP-ZsGreen* mice (P4-P7) were killed by decapitation after deep isoflurane anesthesia. The heads were immersed in ice-cold low-Na^+ cutting solution bubbled with carbogen (a mixture of 95% O_2 and 5% CO_2), and the brains were removed rapidly from the skull. The cutting solution contained the following (in mM): saccharose 205, KCl 2.5, $NaHCO_3$ 26, $MgCl_2$ 5, NaH_2PO_4 1.25, $CaCl_2$ 1, and glucose 10. Hypothalamic blocks were dissected, and 200-μm-thick coronal slices were prepared with a VT-1000S vibratome (Leica Microsystems) in the ice-cold oxygenated cutting solution. Slices including the arcuate nucleus were transferred into aCSF containing (in mM): NaCl 130, KCl 3.5, $NaHCO_3$ 26, $MgSO_4$ 1.2, NaH_2PO_4 1.25, $CaCl_2$ 2.5, and glucose 10 and allowed to equilibrate for 1 h. The aCSF was bubbled with carbogen, and the temperature was allowed to decrease slowly from 33°C to room temperature.

Whole-cell patch-clamp recordings. Recordings were conducted in carbogenated aCSF at 33°C, using an Axopatch-200B patch-clamp amplifier, a Digidata-1322A data acquisition system, and a pCLAMP 10.4 software (Molecular Devices). The patch electrodes (OD = 1.5 mm, thin wall; WPI) were prepared with a Flaming-Brown P-97 puller (Sutter Instrument). Electrode resistance was 2-3 MΩ. The intracellular pipette solution contained the following (in mM): K-gluconate 130, KCl 10, NaCl 10, HEPES 10, $MgCl_2$ 0.1, EGTA 1, Mg-ATP 4, and Na-GTP 0.3. pH 7.2-7.3 with KOH. Osmolarity was adjusted to 300 mOsm with D-sorbitol. To eliminate any direct AR-mediated response to testosterone, the AR blocker flutamide (1 μM; Tocris Bioscience) (Yang et al., 2018) was included in the intracellular pipette solution. Once the whole-cell patch-clamp configuration was achieved, the intracellular milieu was allowed to reach an equilibrium for 15 min before the recording was started. To eliminate indirect transsynaptic actions of testosterone, spike-mediated neurotransmitter release was blocked in all experiments by the addition of the $GABA_A$-R blocker picrotoxin (100 μM, Tocris Bioscience) and the glutamate-receptor blocker kynurenic acid (2 mM, Sigma) to the aCSF 10 min before recording. KP-ZsGreen neurons of the Arc were visualized with a BX51WI IR-DIC microscope (Olympus) placed on an antivibration table (Supertech) using a brief illumination at 470 nm and an epifluorescent filter set. Firing was recorded in current-clamp mode with a holding current of 0 pA. Following a 5 min control recording period, aCSF was replaced with aCSF containing 50 nM T (similar to the male serum T concentration) (Travison et al., 2017; Kapourchali et al., 2020) or 17β-estradiol (E2), and the recording continued for 10 additional minutes. Other measurements were conducted in the presence of the aromatase inhibitor letrozole (100 nM, Tocris Bioscience) (Kretz et al., 2004; Scarduzio et al., 2013) or the broad-spectrum estrogen-receptor antagonist ICI182780 (Faslodex, 1 μM, Tocris Bioscience) (Chu et al., 2009; Balint et al., 2016). The blockers were added to the aCSF 15 min before T (i.e., 10 min before the control recording started) and were present throughout the recording. In some measurements, letrozole was applied intracellularly (100 nM), together with flutamide (1 μM) to eliminate endogenous aromatase activity that might occur within kisspeptin neurons. Each neuron served as its own control when drug effects were evaluated.

Statistical methods. All data are presented as mean ± SEM. Two-tailed unpaired Student's *t* tests were used to determine statistical significance in all counting experiments. Patch-clamp recordings were stored and analyzed offline. Event detection was performed using the Clampfit module of the PClamp 10.4 software (Molecular Devices). Firing rates within the 10 min treatment periods were presented and then illustrated in the bar graphs as percentages of the firing rate of the 5 min control periods (i.e., all experiments were self-controlled in each neuron). Two-tailed unpaired Student's *t* tests were used to determine statistical significance in each group of these percentage firing rate data. The percentage data characterizing the different treatment groups were then compared by ANOVA, followed by Tukey's *post hoc* test. Statistical differences were considered significant at $p < 0.05$.

Table 1. Aromatase neuron distribution in the developing mouse brain[a]

	E13.5		E16.5		E18.5	
Structure	Male	Female	Male	Female	Male	Female
Amygdala						
AhiAL	–	–	–	–	++	++
	–	–	–	–	*	*
Co	–	–	++	++	++	+
	–	–	*	*	**	**
Me	–	–	+++	+++	+++	+++
	–	–	****	****	****	****
opt	–	–	++	++	++	++
	–	–	***	***	***	***
Hypothalamus						
st	+	+	++	++	++	+++
	–	–	****	****	****	****
BNST	–	–	++	++	++	++
	–	–	**	**	***	***
LPO	–	–	+	+	+	++
	–	–	*	*	*	*
LH	–	–	+	+	+	+
	–	–	*	*	*	*
MTu	–	–	+	+	++	+
	–	–	*	*	*	*
MPOA	+	+	+++	+++	++++	++++
	*	*	***	***	***	***
DM	–	–	++	++	++	++
	–	–	**	**	***	***
VM	–	–	++	+	++	++
	–	–	**	**	***	***
PVN	–	–	+	+	++	++
	–	–	**	**	***	***

[a]Cell bodies: +, 0-100; ++, 100-500; +++, 500-1500; ++++, 1500-10,000. Fibers: *Sparse. **Moderate. ***Dense. ****Very dense. -: no signal detected. AHiAL, Amygdalohippocampal area; BNST, bed nucleus of stria terminalis; Co, cortical amygdaloid nucleus; DM, dorsomedial nucleus; LH, lateral hypothalamic area; LPO, lateral preoptic area; Me, medial amygdaloid nucleus; MPOA, medial preoptic area; MTu, medial tuberal nucleus; opt, optic tract; PVN, paraventricular nucleus; st, stria terminalis; VM, ventromedial nucleus.

Results

In utero aromatase expression is initiated in the brain

To identify aromatase neurons in the embryonic mouse brain, we generated reporter mice in which cells activating the promoter of the *Cyp19a1* gene are tagged with τGFP (*ArIC/eR26-τGFP*; Fig. 1*A*). The τGFP fusion protein is actively transported along the axonal microtubules (Mombaerts et al., 1996) visualizing both aromatase-positive perikarya and their projections. While we did not find fluorescent signal in either male or female brains at embryonic day 12.5 (E12.5; Fig. 1*B*), we detected τGFP cells at E13.5 (Fig. 1*C*,*D*; Extended Data Table 1-1). The fluorescent cells were restricted to two distinct forebrain nuclei: the preoptic area (46.0 ± 5.6 τGFP cells in males; 48.8 ± 14.9 cells in females) and the stria terminalis (17.5 ± 4.2 cells in males; 23.1 ± 6.3 cells in females; $n = 4$ or 5 animals), respectively. Both nuclei also contained some τGFP fibers in close apposition to the labeled somata. Of note, fluorescent cells were not apparent in any other tissue of fetuses, demonstrating that *in utero* aromatase expression is restricted to the brain.

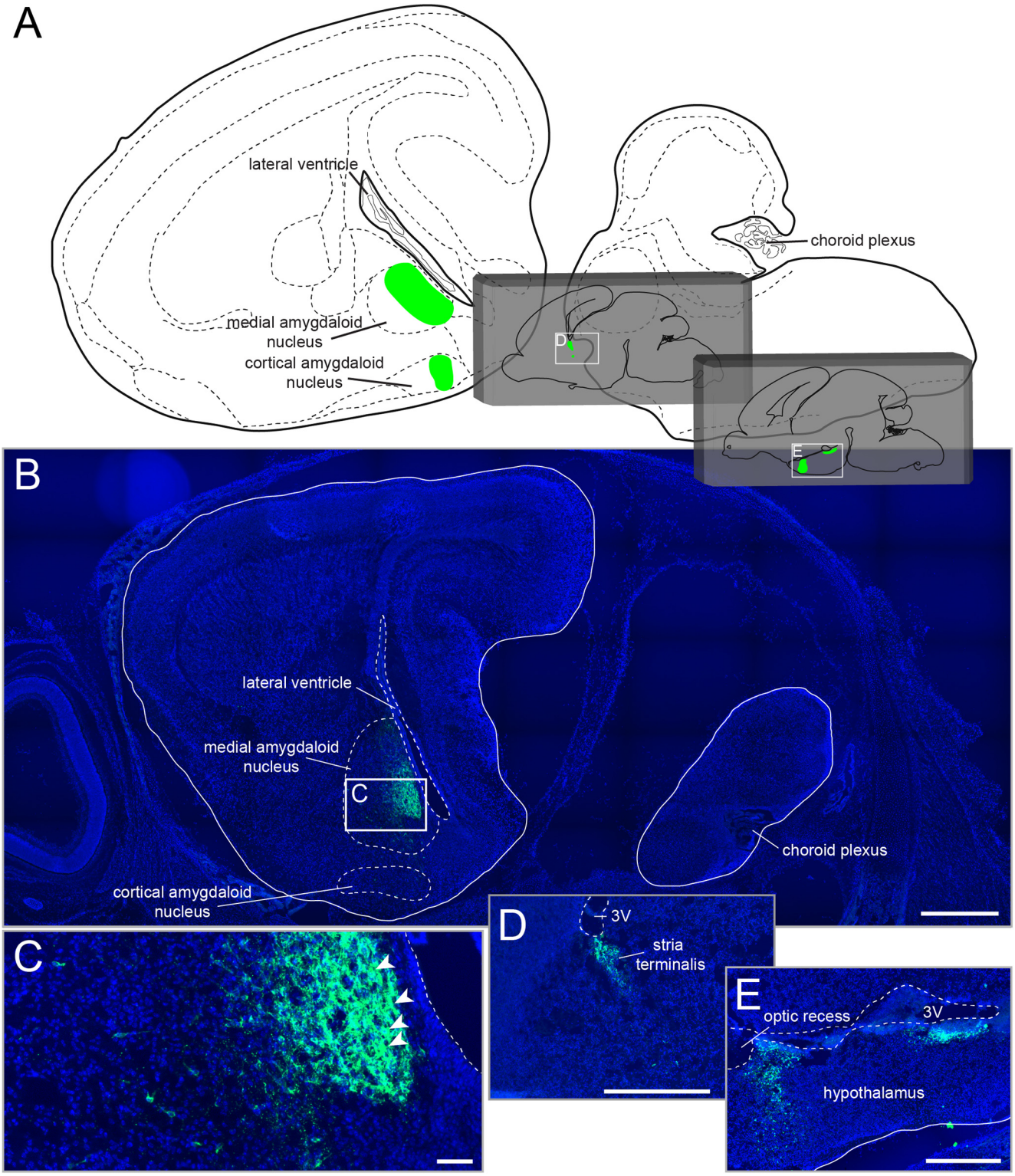

Figure 2. Aromatase expression at E18.5. ***A***, Schematic sagittal overview (Schambra, 2008). Reporter gene expression is restricted to green-labeled areas. Gray insets represent, from lateral to medial, additional schematic sagittal overviews. ***B***, Aromatase expression in the amygdala close to the lateral ventricle. Immunofluorescent analyses showing reporter gene expression (green) and nuclear staining (Hoechst 33258, blue). ***C***, Magnified image of the area indicated in ***B***. White arrowheads indicate labeled somata in close contact with labeled fibers in this nucleus. ***D***, ***E***, Magnified images of the areas indicated in ***A*** (gray insets). Aromatase expression in the stria terminalis (***D***) and in the hypothalamus (***E***). Scale bars: ***B***, ***D***, ***E***, 500 μm; ***C***, 50 μm. 3V, third ventricle.

Development of an embryonic aromatase neural network

The total number of aromatase neurons increased throughout embryonic brain development to >6000 neurons before birth (E13.5: 63.5 ± 6.2 vs E16.5: 3921 ± 380.4 vs E18.5: 6073 ± 324.1 τGFP$^+$ cells in males, $n = 3$-5 animals; and E13.5: 56.3 ± 12.9 vs E16.5: 3330 ± 262.2 vs E18.5: 6583 ± 458.5 cells in females, $n = 3$ or 4 animals; Fig. 1*B*; Table 1). Aromatase expression was restricted to distinct nuclei in the hypothalamus and the amygdala/

stria terminalis at all stages analyzed (Fig. 2). Furthermore, fluorescent cells were not detected in any other embryonic tissues, indicating that *in utero* aromatase expression remains to be restricted to the brain.

At E16.5, most aromatase neurons were identified in the medial amygdaloid nucleus (1047.5 ± 88.8 cells in males, 839.3 ± 83.8 cells in females) and the medial preoptic area (MPOA; 1070.8 ± 178 cells in males, 996.8 ± 70.3 cells in females, $n = 3$ animals) (Fig. 1*B*; Extended Data Table 1-2). Both nuclei were also decorated with extensive fluorescent fibers (Fig. 1*C*,*D*). Additional aromatase neurons were detected in the cortical amygdaloid nucleus and in the optic tract. We also found fluorescent somata and dense fibers in the stria terminalis, the bed nucleus of the stria terminalis, the ventromedial and the dorsomedial nuclei, the paraventricular nucleus, and the medial tuberal nucleus. We detected more τGFP$^+$ neurons in the dorsomedial nucleus in female animals compared with males (unpaired Student's *t* test: $p = 0.0258$; Extended Data Table 1-2). Numerous τGFP fibers were found to be in close contact with other fluorescent somata and/or fibers, suggesting an aromatase neural network (Fig. 1*E*). A few aromatase neurons were located in the lateral preoptic and the lateral hypothalamic areas, respectively.

At E18.5 (Fig. 1*B*,*F*), aromatase expression was picked up in the amygdalohippocampal area (135.8 ± 39.3 cells in males, 150 ± 45.1 cells in females, $n = 3$ animals). A few τGFP fibers were apparent in the amygdalohippocampal area and the cortical amygdaloid nucleus. In contrast, both the optic tract and particularly the medial amygdaloid nucleus contained dense fluorescent fibers, decorating almost the entire nucleus and coming in close contact with numerous aromatase neuron cell bodies (Fig. 1*F*, Table 1; Extended Data Table 1-3). Fluorescent neurons and fibers in the hypothalamus remained restricted to the nuclei identified at E16.5, with somewhat increased cell numbers. Most aromatase neurons were found in the MPOA with 2722.5 ± 123.5 cells in males and 2885 ± 217.4 cells in females ($n = 3$ animals). This individual nucleus also showed the highest increase in tagged cells compared with E16.5 embryos. In the dorsomedial nucleus, more reporter gene-expressing neurons were found in females, comparable to E16.5 animals (unpaired Student's *t* test: $p = 0.0344$; Extended Data Table 1-3). The medial tuberal nucleus, the lateral hypothalamic and the lateral preoptic areas only contained sparse fluorescent fibers, whereas the other τGFP nuclei displayed dense τGFP fibers. The stria terminalis contained particularly dense fluorescent fibers comparable to the medial amygdaloid nucleus. Of note, we did not pick up any gross sexual dimorphism in the aromatase expression pattern in any nucleus at any embryonic developmental stage analyzed (Fig. 1*B*).

To corroborate these findings, we performed qRT-PCR for the *Cyp19a1* gene (catalyzing both the conversion of androstendione to estrone and of T to estradiol) and also for other key enzymes in steroid synthesis, the *Cyp11a1* (converting cholesterol to pregnolone) and *Cyp17a1* genes (converting pregnolone to 17α hydroxypregnolone and to 17α hydroxypregnolone dehyroepiandrosterone), respectively, in E12.5, E13.5, E16.5, and E18.5 animals of both sexes (Fig. 3). We detected very low amounts of *Cyp19a1* mRNA just above the detection threshold at E12.5 and a trend toward some increase at E13.5. *Cyp19a1* expression then increased substantially at E16.5 (E13.5 vs E16.5 unpaired Student's *t* tests: $p = 0.0219$ for females, $p = 0.0064$ for males; $n = 3$ or 4), consistent with higher numbers of aromatase neurons revealed by genetic labeling at this age.

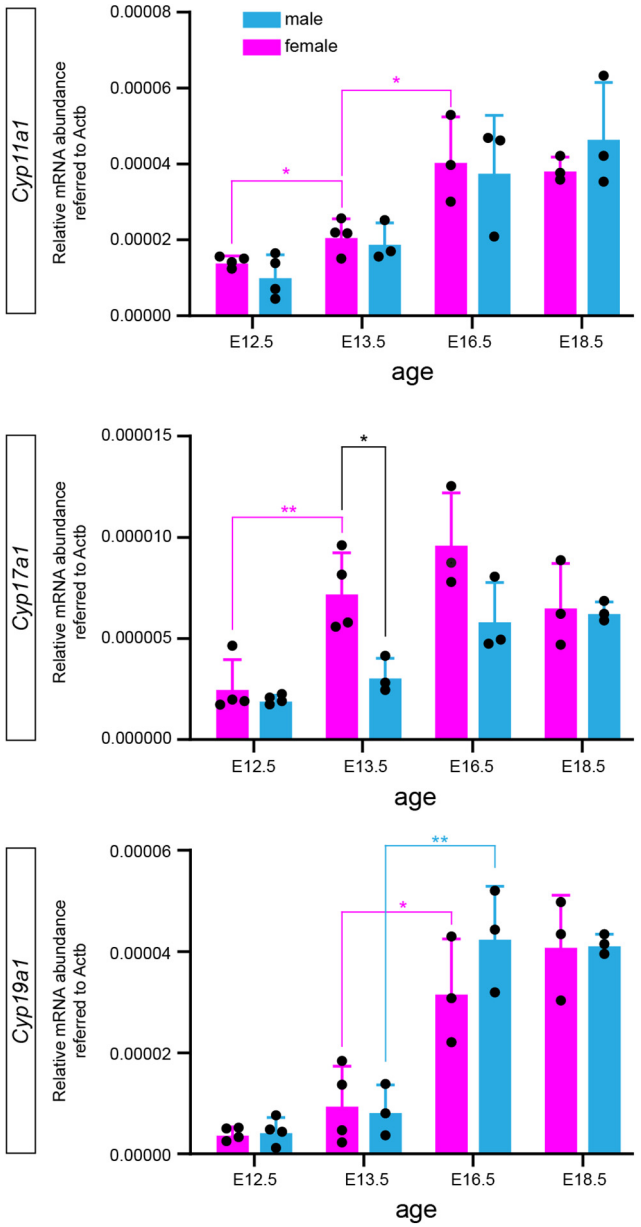

Figure 3. qPCR analyses for *Cyp11a1*, *Cyp17a1*, and *Cyp19a1* mRNAs in the brain of E12.5, E13.5, E16.5, and E18.5 embryos. Note the barely detectable *Cyp19a1* mRNA at E12.5. Except for *Cyp17a1* expression at E13.5, no sexual dimorphism was detected.

Cyp11a1 expression levels increased from E12.5 to E13.5 in females (unpaired Student's *t* test: $p = 0.0872$, $n = 4$), but not in males. Expression increased further at E16.5 (unpaired Student's *t* test: $p = 0.0232$, $n = 3$ or 4) and remained at this plateau at E18.5. *Cyp17a1* expression increased from E12.5 to E13.5 in females (unpaired Student's *t* test: $p = 0.0075$, $n = 4$) with a trend to a further increase at E16.5.

With the sole exception of *Cyp17a1* expression at E13.5, where females expressed more mRNA than males (unpaired Student's *t* test: $p = 0.0195$, $n = 3$ or 4), we did not find age-specific sex differences in expression of these key enzymes in steroid synthesis.

Distinct neural circuits become estrogen-sensitive *in utero*

Aromatase, kisspeptin, GPR54/kisspeptin receptor, and ERα expression all start at E13.5 in the male and female murine brain (Kumar et al., 2014, 2015), suggesting temporal orchestration

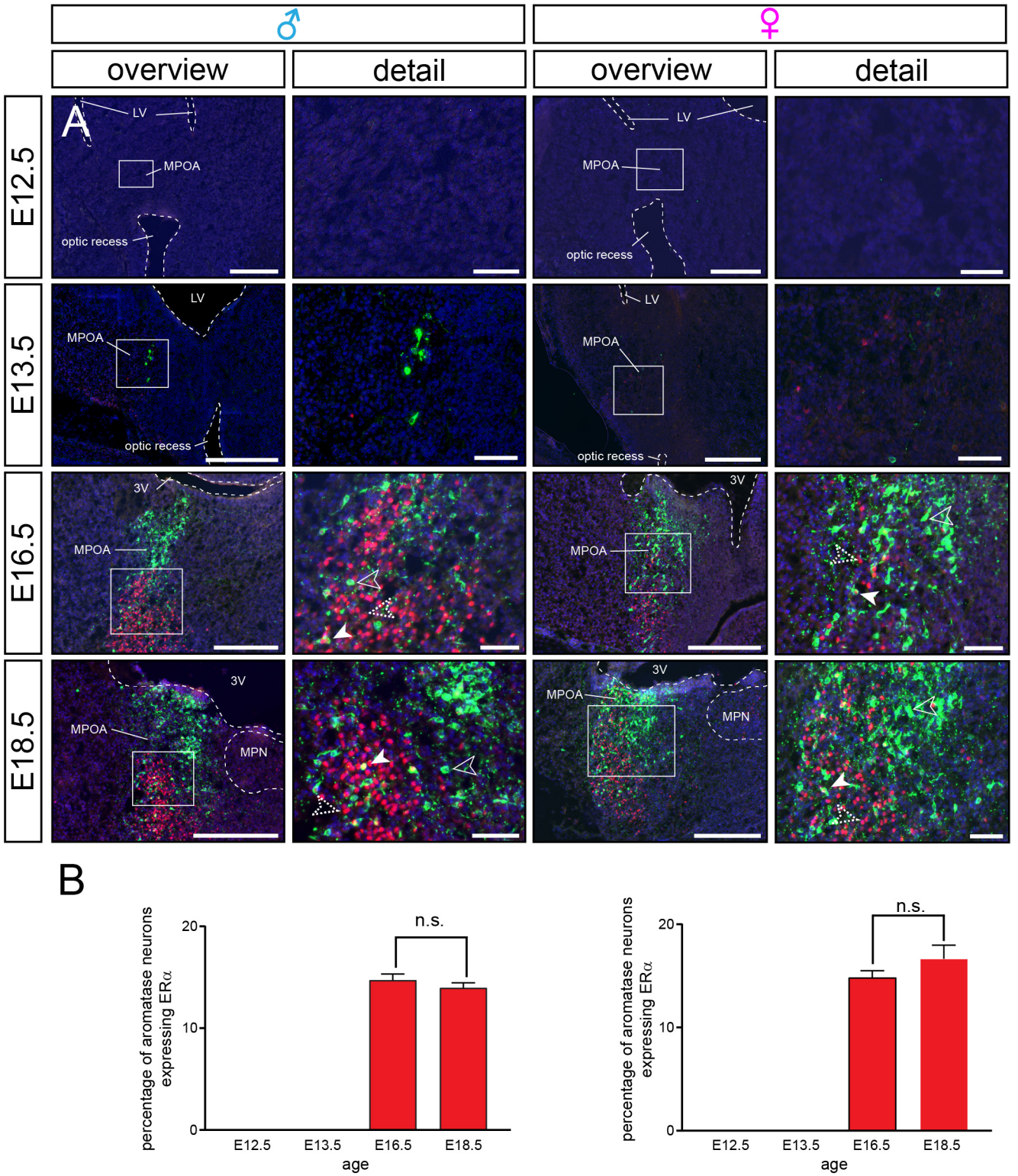

Figure 4. Estrogen-sensitive neural circuits *in utero*. ***A***, Double immunofluorescence for ERα (red) and τGFP (green) of sagittal sections through the MPOA of male and female *ArIC/eR26-τGFP* embryos at different ages. Most male and female aromatase neurons do not express ERα. Nuclear counterstain (Hoechst 33258, blue). Arrowheads indicate aromatase (unfilled), ERα (dotted unfilled), and double-positive neurons (filled). Scale bars: overviews, 250 µm; details, 50 µm. 3V, third ventricle; LV, lateral ventricle; MPN, median preoptic nucleus. ***B***, Quantification of ERα expression in aromatase neurons in male and female embryos. Detailed double-positive cell numbers and ratios for each nucleus are reported in Extended Data Tables 4-1, 4-2, and 4-3.

and raising the possibility that locally produced neurosteroids impinge onto estrogen-sensitive neural circuits *in utero*. To characterize the respective circuitry and test whether estrogen sensitivity may provide an autocrine feedback mechanism in aromatase neurons, we immunolabeled sections prepared from ArIC/eR26-τGFP brains with antibodies against ERα. We focused on ERα in this study as it has been shown to play a major role in the development and regulation of the reproductive axis (Walker and Korach, 2004; Mayer et al., 2010). We did not detect immunofluorescence signals for ERα in E12.5 embryos

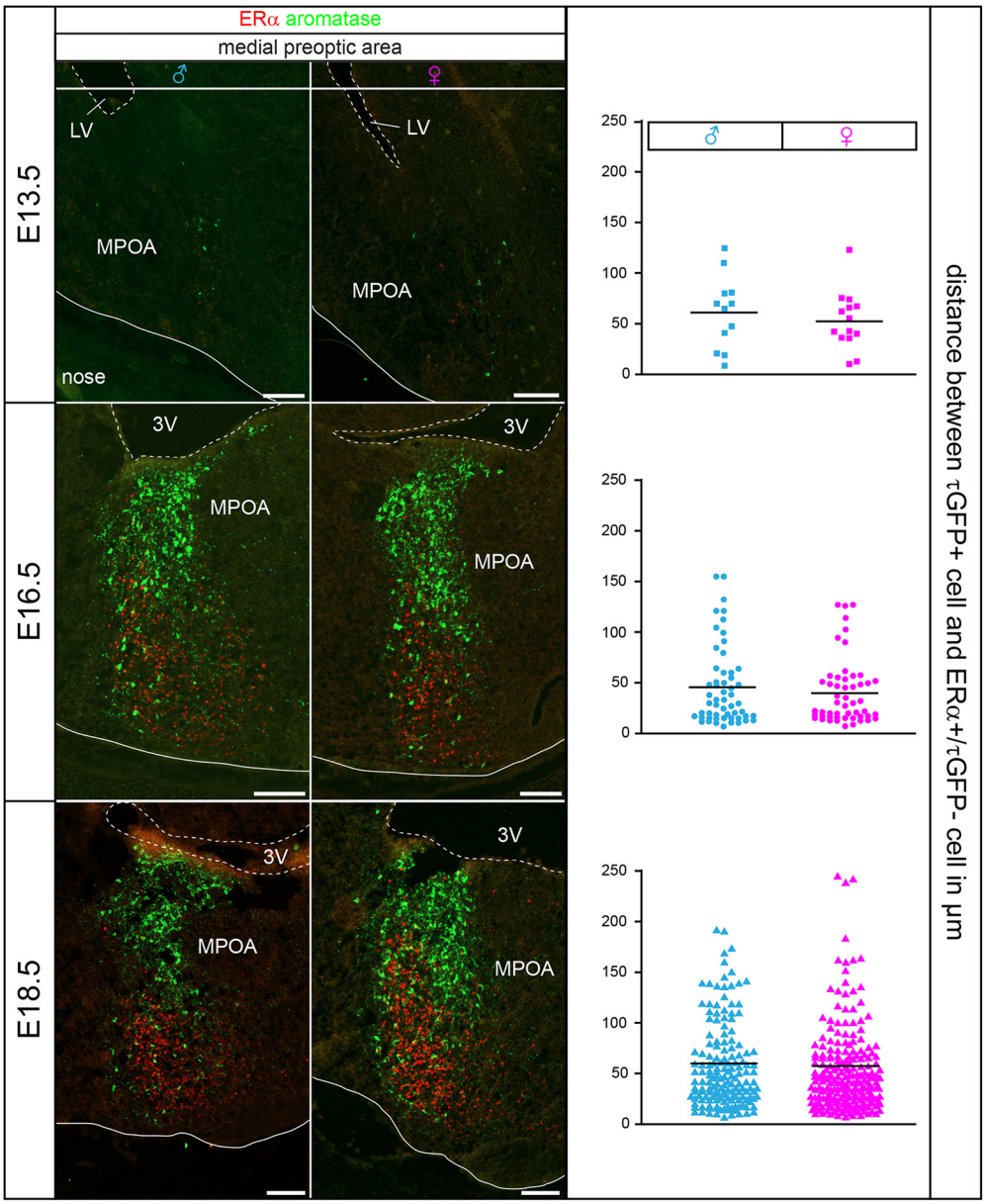

Figure 5. Close proximity of aromatase neurons to estrogen-sensitive circuits. Double immunofluorescence for ERα (red) and τGFP (green) of sagittal sections through the MPOA of male and female *ArlC/eR26-τGFP* embryos at different ages. Graphs represent the distance between aromatase and ERα neurons. Scale bars, 100 µm. 3V, third ventricle; LV, lateral ventricle.

(Fig. 4), consistent with previous reports (Kumar et al., 2014, 2015). While ERα immunoreactivity was apparent in multiple nuclei at E13.5, it did not colocalize with aromatase neurons in females or in males (Fig. 4; Extended Data Table 4-1). In contrast, ~15% (14.7 ± 0.6% in males, 14.8 ± 0.7% in females, $n = 3$ animals) of all aromatase neurons expressed ERα at E16.5. Specifically, some colocalization between aromatase and ERα signals was picked up in the amygdala, the optic tract, and the stria terminalis, while we did not observe ERα expression in most hypothalamic aromatase neurons.

The medial tuberal nucleus exhibited the highest colocalization rate (57.1 ± 12% in males, 44.4 ± 3.2% in females) but contained only few aromatase neurons (Extended Data Table 4-2). Vice versa, the MPOA with the highest number of aromatase neurons only showed a low rate of colocalization (11.4 ± 1.6% in males, 7.6% ± 3.2 in females).

ERα-positive aromatase neurons remained at similarly low frequency at E18.5 (14 ± 0.5% of aromatase neurons in males, 16.7 ± 1.3% in females; Extended Data Table 4-3). For example, while we did observe intense ERα staining in the optic tract, we found that hardly any τGFP somata overlapped with the ERα population. ERα-positive aromatase neurons increased somewhat in total numbers compared with E16.5 (unpaired Student's *t* tests: $p = 0.0168$ for males and $p = 0.0051$ for females; Extended Data Tables 4-2 and 4-3). Together, these data suggest little autocrine estrogen action on aromatase neurons in the embryonic mouse brain via ERα.

Aromatase neurons are in close proximity to estrogen-sensitive circuits

We next investigated the spatial relationship between aromatase and estrogen-sensitive neurons and determined the mean

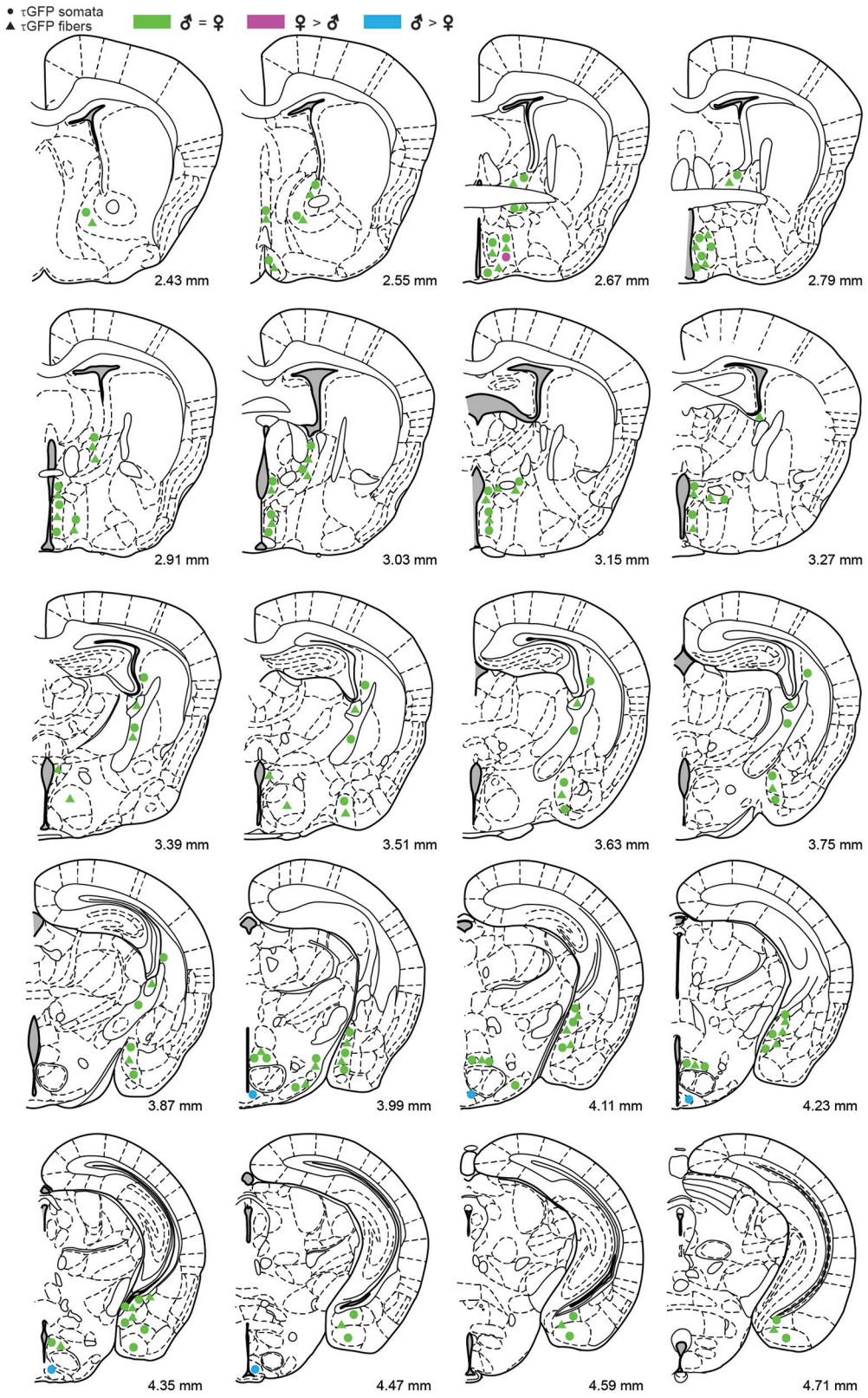

Figure 6. Summary of reporter gene expression in the P0 brain. Schematic coronal representations taken from Paxinos et al. (2007). Distances (in mm) from the most rostral section of the atlas are indicated. Green circles and triangles represent areas with similar numbers of cell bodies and fibers, respectively, in males and females. Blue symbols represent areas with more cell bodies and fibers in males. Pink symbols represent areas with more cell bodies and fibers in females. No reporter gene expression was detected in more rostral or caudal sections. Detailed cell number counts are presented in Extended Data Tables 6-1 and 6-2.

distance between these cells in the MPOA of the hypothalamus. We found average distances corresponding to ~2-3 cell diameters between aromatase and ERα neurons (61.4 µm in males and 50.9 µm in females at E13.5, 44.6 µm in males and 38.9 µm in females at E16.5, 55.2 µm in males and 50.1 µm in females at E18.5). Similar distances were determined in the medial amygdaloid nucleus (26.4 µm in males and 25.9 µm in females at E16.5, 47.4 µm in males and 42.9 µm in females at E18.5). Together, these data demonstrate that most aromatase neurons are in close proximity to estrogen-sensitive neurons in the embryonic mouse brain and raise the possibility that locally synthesized estrogen acts on adjacent ERα-positive but aromatase-negative cells (Fig. 5).

Sexually dimorphic aromatase expression in the arcuate nucleus at birth

Aromatase expression at P0 remained restricted to nuclei of the amygdala and hypothalamus. We detected more aromatase neurons in the female MPOA (unpaired Student's *t* test: 0.0418) (Fig. 6; Extended Data Table 6-1). Colocalization rates between aromatase neurons and ERα neurons in P0 animals were also similar to embryonic brains with the majority of nuclei showing no sex differences. Exceptions were the medial division, posteromedial part of the bed nucleus of stria terminalis (26.44 ± 4.14% in females and 3.81 ± 2.23% in males, unpaired Student's *t* test: $p = 0.0018$), the medial amygdaloid nucleus, posterodorsal part (43.83 ± 8.66% in females and 9.52 ± 3.13% in males, unpaired Student's *t* test: $p = 0.0390$), and the posteromedial cortical amygdaloid nucleus (11.80 ± 4.59% in females and 2.66 ± 1.60% in males, unpaired Student's *t* test: $p = 0.0390$; Extended Data Table 6-2).

To test the hypothesis that aromatase neurons may act as local producers of estrogen and to determine whether neurosteroids act on reproductive neural circuits just after birth, we analyzed the spatial relationship between aromatase and kisspeptin neurons. Kisspeptin neurons are restricted to the arcuate nucleus of the hypothalamus until puberty and express ERα (Kumar et al., 2014, 2015). We did not detect aromatase neurons in the arcuate nucleus in either males or females throughout embryonic development (Fig. 7; Extended Data Figs. 7-1 and 7-2).

However, this changed at birth (Fig. 6). At P0, we found a cluster of τGFP neurons in the male arcuate nucleus (176 ± 64.1 τGFP cells, $n = 5$ animals; Extended Data Table 6-1). This aromatase neuron cluster was notably absent in the female arcuate nucleus, demonstrating sexually dimorphic aromatase expression in this area of the hypothalamus at birth.

We next stained brains sections prepared from ArIC/eR26-τGFP brains with antibodies against kisspeptin. While none of the arcuate aromatase neurons expressed kisspeptin (Fig. 8*A*), these two neuronal subtypes were always in the immediate vicinity of each other, suggesting steroid hormone action on kisspeptin neurons in the male mouse brain at birth (Fig. 9).

Inhibition of arcuate kisspeptin neurons by T requires estrogen production by aromatase neurons

We hypothesized that aromatase neurons in the developing brain generate neuroestrogens from brain-born and/or circulating androgens to regulate the activity of the adjacent estrogen-sensitive cells. To test this hypothesis, we used electrophysiology on acute brain slice preparations comprising the arcuate nucleus from newborn (P4-P7) male and female mice with genetically labeled kisspeptin neurons. We conducted whole-cell patch-clamp experiments in current-clamp mode to record the firing of

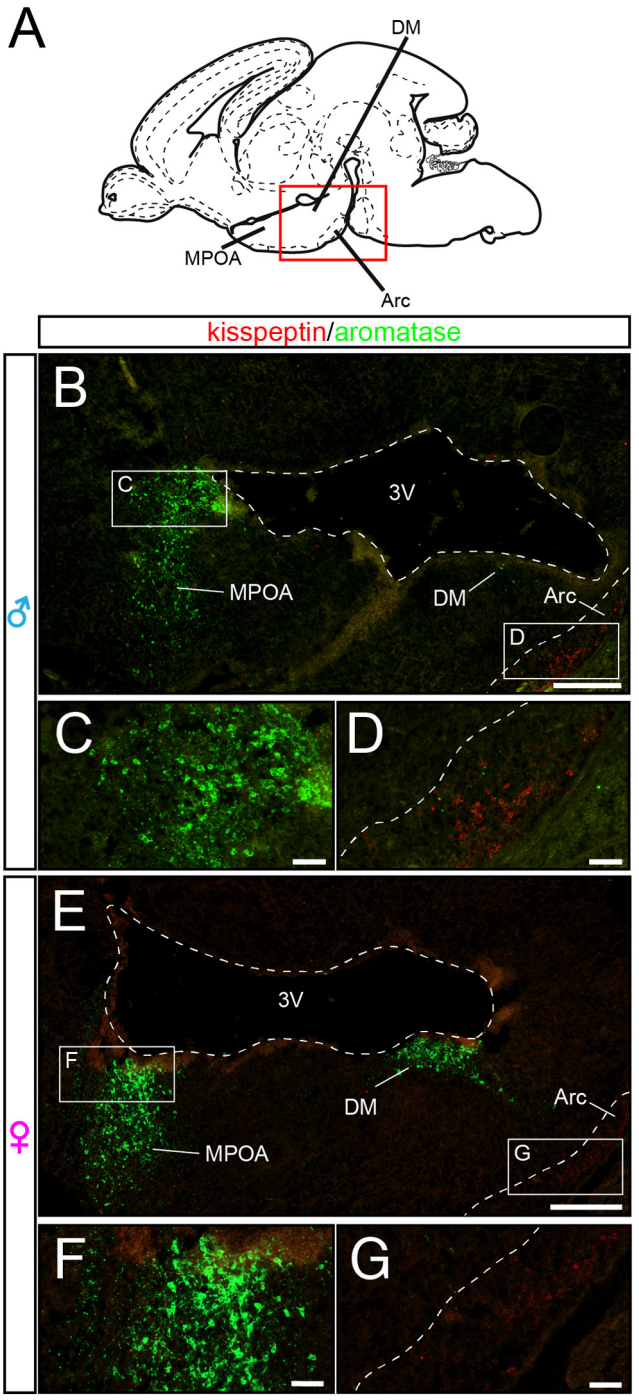

Figure 7. Aromatase and kisspeptin expression in distinct nuclei of the hypothalamus and amygdala at E18.5. ***A***, Schematic sagittal overview of the regions shown in ***B–G***. Arc, Arcuate nucleus; DM, dorsomedial nucleus. ***B–G***, Double immunofluorescence for kisspeptin (red) and τGFP (green). Aromatase is not expressed in the embryonic Arc (Extended Data Figures 7-1 and 7-2), delineated by kisspeptin labeling (Kumar et al., 2014). 3V, third ventricle. ***B***, Sagittal section through the hypothalamus of a male embryo at E18.5. ***C***, Reporter expression in the MPOA. ***D***, Arc. ***E–G***, Aromatase and kisspeptin expression in females. Scale bars: ***B–F***, overview, 250 µm; inset, 50 µm. Schematic reference picture taken from Schambra (2008).

fluorescent kisspeptin neurons expressing ZsGreen. Indirect transsynaptic actions of T were eliminated by including picrotoxin and kynurenic acid in the aCSF. We also added the AR antagonist flutamide (100 nM) to the electrode solution to block AR-mediated direct responses of the recorded kisspeptin neuron to T. As most kisspeptin neurons showed no spontaneous

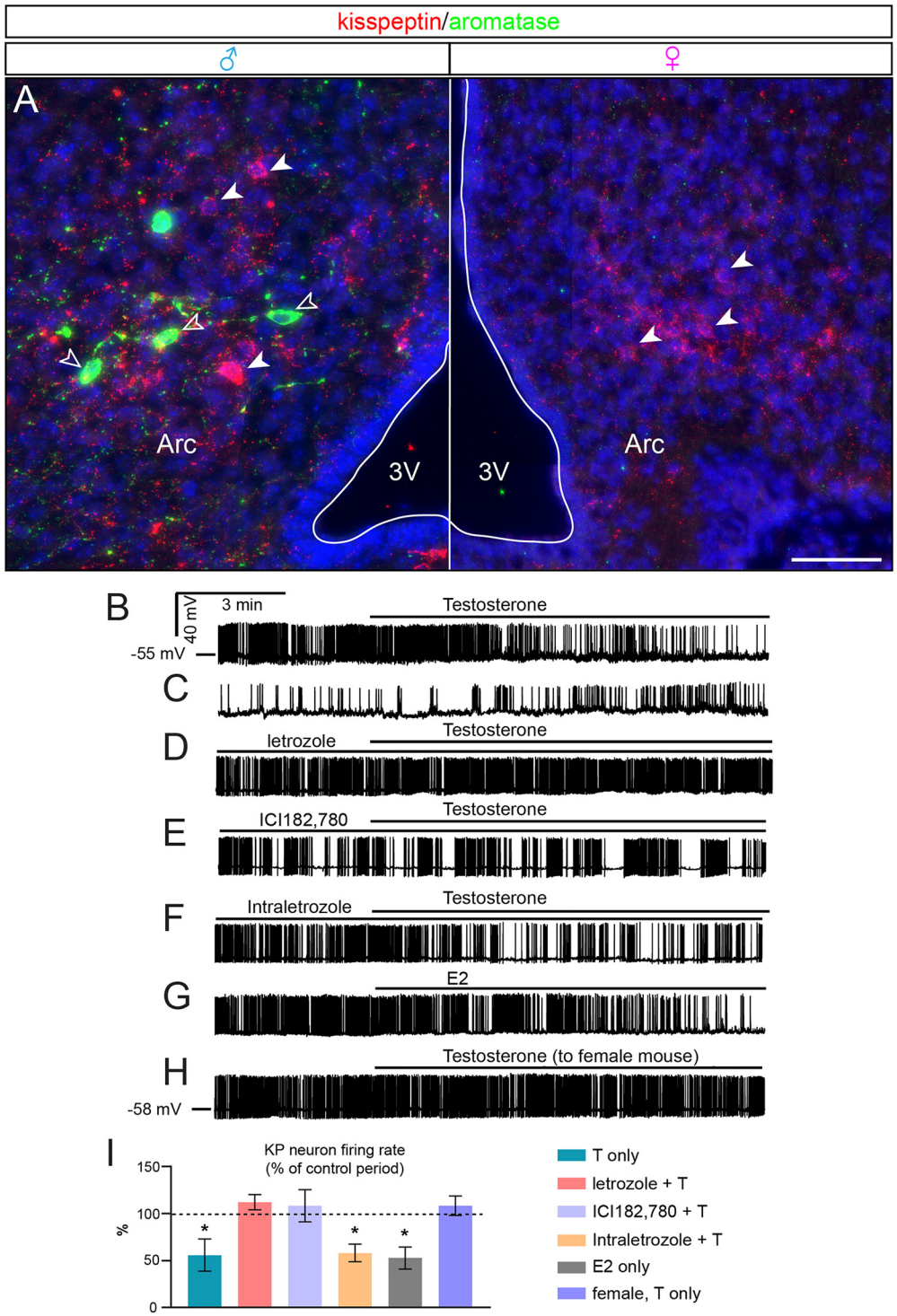

Figure 8. Sexually dimorphic aromatase expression in the arcuate nucleus (Arc) and direct actions of T on kisspeptin neuron firing. ***A***, Reporter gene expression was only detected in the male Arc after birth. Arcuate aromatase is not expressed in kisspeptin neurons. Arrowheads indicate kisspeptin (filled) and aromatase (unfilled) neurons, respectively. 3V, Third ventricle. ***B–H***, Representative traces recorded from kisspeptin neurons in the male (***B–G***) and female (***H***) Arc. ***B***, Decreased firing rate in response to T administration. ***C***, The effect of T could be washed out slowly. ***D***, Presence of letrozole in the extracellular solution prevented the action of T. ***E***, The ER antagonist ICI182780 also abolished the action of T. ***F***, Intracellular administration of letrozole showed no antagonistic effect, unlike its extracellular use in ***D***. ***G***, Mimicking the effect of T, E2 reduced arcuate kisspeptin neuron firing in males. ***H***, T had no effect on the firing of kisspeptin neurons in females, which lack arcuate aromatase neurons. For experimental details, see main text. ***I***, T reduced kisspeptin neuron firing in males only. This action was entirely prevented by prior bath application of the aromatase inhibitor letrozole or the ER inhibitor ICI182780, indicating that T conversion to E2 and ERs plays a role in the effect of T. Estradiol was not derived from the recorded kisspeptin neurons because letrozole in the electrode solution (intra letrozole) did not interfere with T actions. T only, $p = 0.0242$; intra letrozole + T, $p = 0.0025$; E2 only, $p = 0.0091$ by Student's t tests. For detailed statistics, see Extended Data Tables 8-1, 8-2, and 8-3. Scale bars, 50 μm.

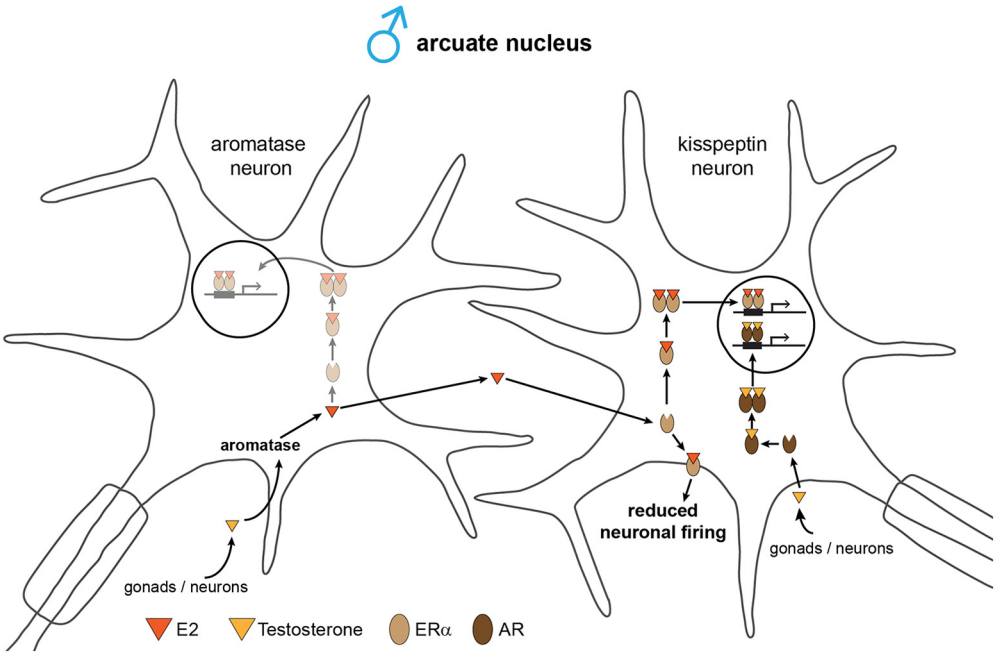

Figure 9. Model of estrogenic actions on kisspeptin neurons in the male arcuate nucleus. Testosterone, either of gonadal or neuronal origin, is converted by arcuate aromatase neurons to E2 and acts on membrane-bound ERα in adjacent kisspeptin neurons reducing their neuronal firing rate. Both T and E2 could also exert genomic effects via nuclear AR and ERα in kisspeptin neurons. Because a small subset of aromatase neurons expresses ERα, E2 could also exert genomic effects in these cells.

activity, a 10 pA depolarizing current was applied during the entire recording period to induce and maintain firing. Firing of kisspeptin neurons ($n = 33$) was typically irregular with frequent burst-like patterns and 3- to 5-min-long oscillations between peaks and nadirs. This observation fitted well with the activity patterns reported for adult mice (Clarkson et al., 2017; Vanacker et al., 2017). The mean firing rate during the 5 min control period was 2.26 ± 0.54 Hz ($n = 7$ cells) but decreased significantly following T administration (50 nM) to $54.1 \pm 15.3\%$ of the control rate (Student's t test, $p = 0.0242$) (Fig. 8*B*, *I*, first column; Extended Data Table 8-1). Neuronal activity started to decline 3.4 ± 1.1 min after T application to the aCSF. A washout effect was reflected in the slow increase in neuronal activity 15-20 min after T treatment was suspended (Fig. 8*C*). The reduced firing rate of kisspeptin neurons in response to T treatment resembled the estrogen response of adult kisspeptin neurons (Cholanian et al., 2014; Ruka et al., 2016).

This resemblance and the absence of detectable aromatase signal in kisspeptin neurons (see above) raised the possibility that T requires conversion to estradiol by aromatase neurons to inhibit kisspeptin neuron firing. Therefore, we replicated the above experiment with both T and the aromatase inhibitor letrozole (100 nM) in the aCSF. Following a 5 min control period with letrozole in the aCSF, the recording was continued for 10 min in the presence of T. Preincubation of the slice with letrozole completely prevented the effect of T on kisspeptin neuron firing ($112.0 \pm 8.16\%$ of the control value 1.8 ± 0.48 Hz, Student's t test, $p = 0.2029$, $n = 6$ cells) (Fig. 8*D*, *I*, second column; Extended Data Table 8-1). This observation indicated that T needs to be converted to estradiol by aromatase to act on ERs in kisspeptin neurons. Indeed, T was unable to alter kisspeptin neuron activity in the presence of the ER inhibitor ICI182780 ($108.5 \pm 16.92\%$ of the control value 1.8 ± 0.21 Hz, Student's t test, $p = 0.632$, $n = 8$ cells) (Fig. 8*E*, *I*, third column; Extended Data Table 8-1). Although aromatase neurons do not seem to express kisspeptin in our immunohistochemical analyses, a recent RT/PCR study reported the presence of the aromatase transcript in pooled kisspeptin neurons of the developing murine arcuate nucleus (Alfaia et al., 2019). To rule out that T is converted to estradiol by a low level of endogenous aromatase in these cells and to prove that T acts mostly indirectly on kisspeptin neurons, letrozole (100 nM), in addition to flutamide, was added to the electrode solution and then the effect of T reassessed. T application in this study resulted in a significant decrease in kisspeptin neuron firing ($57.7 \pm 9.24\%$ of the control value 1.9 ± 0.31 Hz, Student's t test, $p = 0.0025$, $n = 8$ cells) (Fig. 8*F*, *I*, fourth column; Extended Data Table 8-1), which was similar to the effect of T alone (Fig. 8*I*, first column).

This observation indicated that endogenous aromatase has only minor, if any, contribution to the T effect on kisspeptin neuron firing; therefore, the mechanism whereby T acts on kisspeptin neurons is via aromatization in other neurons. To confirm the key role of E2 in the inhibition of arcuate kisspeptin neurons on T administration, we replaced T with an equimolar concentration of E2 in the next experiment. Administration of 50 nM E2 evoked a substantial decrease in the firing rate of kisspeptin neurons ($52.7 \pm 11.47\%$ of the control value of 1.98 ± 0.21 Hz, Student's t test, $p = 0.0091$, $n = 6$ cells) (Fig. 8*G*, *I*, fifth column; Extended Data Table 8-1), mimicking the effect of T.

If arcuate aromatase neurons account for the conversion of T to E2 in males, we hypothesized that T would not produce the same effect in females which lack aromatase neurons in the arcuate nucleus. Indeed, T did not affect the firing rate of arcuate nucleus kisspeptin neurons in newborn female mice ($112.2 \pm 8.11\%$ of the control value of 2.02 ± 0.19 Hz, Student's t test, $p = 0.1936$, $n = 6$ cells) (Fig. 8*H*, *I*, sixth column; Extended Data Table 8-1).

The firing rates of the different treatment groups were significantly different by ANOVA ($p = 0.0006$) followed by Tukey's *post hoc* test (T only vs letrozole + T, $p = 0.0379$; T only vs ICI182780 + T, $p = 0.0351$; T only vs T to female, $p = 0.0369$; letrozole + T vs intra letrozole + T, $p = 0.0484$; letrozole +

T vs E2 only, $p = 0.0414$; ICI182780 + T vs intra letrozole + T, $p = 0.0448$; ICI182780 + T vs E2 only, $p = 0.0396$; intra letrozole + T vs T to female, $p = 0.0471$; E2 only vs T to female, $p = 0.0404$; Extended Data Table 8-2). Analysis of the control periods (before T) with ANOVA followed by Tukey's *post hoc* test showed that ICI182780 or intra/extracellular letrozole alone did not alter the firing rate (ANOVA, $p = 0.9395$; Extended Data Table 8-3).

Discussion

To gain insight into how the maturation of the reproductive axis may be influenced by neurosteroid signaling, we used a genetic approach to analyze the development of the aromatase neuronal network in the embryonic and perinatal murine brain. Our data reveal the following: (1) Neuronal aromatase expression starts at E13.5 in two distinct forebrain nuclei. (2) The number of aromatase neurons increases substantially until birth, but aromatase expression remains restricted to the hypothalamus and the amygdala. (3) There is no obvious major sexual dimorphism in the number and projections of aromatase neurons in the embryonic brain. (4) Most aromatase neurons do not express ERα but (5) are in close proximity to ERα neurons, suggesting mostly local actions of neuroestrogens. (6) At birth, a cluster of aromatase neurons in the hypothalamic arcuate nucleus adjacent to kisspeptin neurons becomes apparent in males, but not in females. (7) Aromatase neurons communicate gonadal and/or brain-derived androgen signals to adjacent estrogen-sensitive neurons. Specifically, arcuate aromatase neurons in perinatal males convert T to estradiol, which reduces kisspeptin neuron firing via rapid actions on ERs. Together, our data provide a cellular substrate underlying aromatase action in the developing murine brain.

Conclusive experimental evidence documenting aromatase expression in the embryonic brain at a cellular resolution had been difficult to obtain. We found the first activity of the *Cyp19a1* promoter to be restricted to a few neurons in two distinct areas of the hypothalamus, possibly explaining the difficulties in previous experimental attempts trying to demonstrate steroid hormone production in the brain *in utero*. Aromatase expression as visualized with high sensitivity in the reporter mice is very selective and highly similar if not stereotyped in between age-matched individuals, arguing against a random stochastic activation of the promoter in this animal model. The onset of aromatase expression in the reporter mice coincides with the first ERα expression in distinct hypothalamic neurons (Kumar et al., 2014, 2015), suggesting that the brain becoming estrogen-sensitive may be orchestrated with the potential *de novo* synthesis of neurosteroids. Notably, the first aromatase-expressing cells in the entire embryo originate in the brain and not in the gonads or anywhere else. Aromatase neurons remain restricted to a few nuclei in the hypothalamus and the amygdala during embryogenesis, without obvious major differences between males and females. One caveat we need to consider is that sex differences in aromatase activity within individual aromatase neurons are not reported by the genetic labeling approach and may thus have escaped our analyses. qPCR measurements of mRNA levels did not reveal major differences between sexes. Most aromatase neurons do not express ERα during embryogenesis but are in close proximity to estrogen-sensitive cells. These data raise the possibility that local neuroestrogen action resulting from *de novo* synthesis and/or conversion might play an active role other than sexual differentiation in the embryonic brain, for example, in neural differentiation (Toran-Allerand, 1976). Consistent with this, some estradiol has indeed been detected in the embryonic rat brain using radioimmune assays (Konkle and McCarthy, 2011), and estrogens were shown to promote neurite growth in the developing brain *in vitro* (Toran-Allerand et al., 1983) and in cultured fetal neurons (Carrer et al., 2005). Fetal *de novo* neurosteroid synthesis is also in line with our finding that the mRNAs of at least three key enzymes of steroid synthesis are expressed in the brain before birth. Together, our data demonstrate that an aromatase neuronal network consisting of well over 6000 neurons develops in both male and female embryos long before the well-documented masculinizing and feminizing actions of estrogen.

The classical aromatization hypothesis states that the female brain is the default brain and that estrogen is not needed during early development (females are protected by α-fetoprotein). Accordingly, feminizing estrogen actions start postnatally (i.e., when the ovaries start to produce estradiol). Consistent with this, significant amounts of serum estrogen were not detected in female rats before P7 (Lamprecht et al., 1976). Male brains are masculinized and defeminized by estrogen aromatized from circulating T originating from the testis in later developmental stages. In contrast, our results suggest that the brain relies on estrogenic actions starting in the embryo. Because we did not detect gross sex differences in the aromatase neuronal network *in utero* in either cell numbers or mRNA expression, we propose that neuroestrogens act both in the male and female embryonic brain to establish a "default" brain status before undergoing sexual differentiation later in development (i.e., when circulating estrogen levels rise in females or subsequent to the T surge in males) (Baum et al., 1991). Our data predict that fetal neuroestrogens act mainly locally, possibly even in a paracrine manner, within distinct nuclei in the hypothalamus and the amygdala.

Aromatase and estrogen-sensitive neurons are found in close proximity, indicating that estrogen is only partially acting as a hormone but rather like a neurotransmitter. Hormones are typically released far away from their site of action and exert long-lasting effects, such as changing gene expression. Neurotransmitters, on the other hand, act close to their release site, and their effects typically occur within milliseconds (Balthazart and Ball, 2006). One prerequisite for estrogen to act as a neurotransmitter is that its synthesis and release need to be regulated within a much shorter time span than the modulation of aromatase expression levels would permit. Consistent with this, aromatase activity can be blocked by phosphorylation of two residues in the aromatase enzyme in a Ca^{2+}-dependent manner (Balthazart et al., 2001), providing a mechanism to switch off estrogen synthesis within milliseconds. In birds, aromatase was localized in axon terminals (Balthazart and Ball, 2006). We detected dense, nucleus-dependent aromatase fibers in the embryonic ArIC/eR26-τGFP brains. If aromatase is also located in the axon terminal in rodents, aromatase neurons could exert neurotransmitter-like estrogen actions far away from their cell body. Neurosteroids may act as local signaling cues that act shortly and rapidly on neighboring cells (Kow and Pfaff, 2004; Cornil et al., 2006). We found that T reduced the firing rate of male kisspeptin neurons. One reason why kisspeptin neuron activity needs to be suppressed during the neonatal period is to silence the reproductive axis (i.e., the GnRH/luteinizing hormone pulse generator) until puberty onset to allow proper sexual maturation. In addition to its membrane effect, neuroestrogens might also influence gene expression in adjacent estrogen-sensitive neurons, mediated by ERα acting as a transcription factor. Future experiments will be aimed at delineating the connectivity map of aromatase neurons and assign neurosteroid function to the individual aromatase-expressing nuclei.

References

Agulnik AI, Bishop CE, Lerner JL, Agulnik SI, Solovyev VV (1997) Analysis of mutation rates in the SMCY/SMCX genes shows that mammalian evolution is male driven. Mamm Genome 8:134–138.

Alfaia C, Robert V, Poissenot K, Levern Y, Guillaume D, Yeo S, Colledge W, Franceschini I (2019) Sexually dimorphic gene expression and neurite sensitivity to estradiol in fetal arcuate Kiss1 cells. J Endocrinol 18:e13002.

Bakker J, De Mees C, Douhard Q, Balthazart J, Gabant P, Szpirer J, Szpirer C (2006) Alpha-fetoprotein protects the developing female mouse brain from masculinization and defeminization by estrogens. Nat Neurosci 9:220–226.

Balint F, Liposits Z, Farkas I (2016) Estrogen receptor beta and 2-arachidonoylglycerol mediate the suppressive effects of estradiol on frequency of postsynaptic currents in gonadotropin-releasing hormone neurons of metestrous mice: an acute slice electrophysiological study. Front Cell Neurosci 10:77.

Balthazart J (2020) Sexual partner preference in animals and humans. Neurosci Biobehav Rev 115:34–47.

Balthazart J, Ball GF (2006) Is brain estradiol a hormone or a neurotransmitter? Trends Neurosci 29:241–249.

Balthazart J, Foidart A, Surlemont C, Harada N (1991) Distribution of aromatase-immunoreactive cells in the mouse forebrain. Cell Tissue Res 263:71–79.

Balthazart J, Baillien M, Ball GF (2001) Phosphorylation processes mediate rapid changes of brain aromatase activity. J Steroid Biochem Mol Biol 79:261–277.

Baum MJ, Woutersen PJ, Slob AK (1991) Sex difference in whole-body androgen content in rats on fetal days 18 and 19 without evidence that androgen passes from males to females. Biol Reprod 44:747–751.

Boehm U, Zou Z, Buck LB (2005) Feedback loops link odor and pheromone signaling with reproduction. Cell 123:683–695.

Candlish M, Wartenberg P, Boehm U (2018) Genetic strategies examining kisspeptin regulation of GnRH neurons. In: The GnRH neuron and its control (Allan H, ed). pp 259–287. Hoboken, NJ: Wiley Blackwell.

Carrer HF, Cambiasso MJ, Gorosito S (2005) Effects of estrogen on neuronal growth and differentiation. J Steroid Biochem Mol Biol 93:319–323.

Cholanian M, Krajewski-Hall SJ, Levine RB, McMullen NT, Rance NE (2014) Electrophysiology of arcuate neurokinin B neurons in female Tac2-EGFP transgenic mice. Endocrinology 155:2555–2565.

Chu Z, Andrade J, Shupnik MA, Moenter SM (2009) Differential regulation of gonadotropin-releasing hormone neuron activity and membrane properties by acutely applied estradiol: dependence on dose and estrogen receptor subtype. J Neurosci 29:5616–5627.

Clarkson J, Han SY, Piet R, McLennan T, Kane GM, Ng J, Porteous RW, Kim JS, Colledge WH, Iremonger KJ, Herbison AE (2017) Definition of the hypothalamic GnRH pulse generator in mice. Proc Natl Acad Sci USA 114:E10216–E10223.

Cornil CA, Taziaux M, Baillien M, Ball GF, Balthazart J (2006) Rapid effects of aromatase inhibition on male reproductive behaviors in Japanese quail. Horm Behav 49:45–67.

De Mees C, Bakker J, Szpirer J, Szpirer C (2007) Alpha-fetoprotein: from a diagnostic biomarker to a key role in female fertility. Biomark Insights 1:82–85.

Dubois SL, Acosta-Martinez M, DeJoseph MR, Wolfe A, Radovick S, Boehm U, Urban JH, Levine JE (2015) Positive, but not negative feedback actions of estradiol in adult female mice require estrogen receptor alpha in kisspeptin neurons. Endocrinology 156:1111–1120.

Dubois SL, Wolfe A, Radovick S, Boehm U, Levine JE (2016) Estradiol restrains prepubertal gonadotropin secretion in female mice via activation of ERalpha in kisspeptin neurons. Endocrinology 157:1546–1554.

Glanowska KM, Venton BJ, Moenter SM (2012) Fast scan cyclic voltammetry as a novel method for detection of real-time gonadotropin-releasing hormone release in mouse brain slices. J Neurosci 32:14664–14669.

Kapourchali FR, Louis XL, Eskin MN, Suh M (2020) A pilot study on the effect of early provision of dietary docosahexaenoic acid on testis development, functions, and sperm quality in rats exposed to prenatal ethanol. Birth Defects Res 112:93–104.

Kenealy BP, Kapoor A, Guerriero KA, Keen KL, Garcia JP, Kurian JR, Ziegler TE, Terasawa E (2013) Neuroestradiol in the hypothalamus contributes to the regulation of gonadotropin releasing hormone release. J Neurosci 33:19051–19059.

Kenealy BP, Keen KL, Garcia JP, Kohlenberg LK, Terasawa E (2017) Obligatory role of hypothalamic neuroestradiol during the estrogen-induced LH surge in female ovariectomized rhesus monkeys. Proc Natl Acad Sci USA 114:13804–13809.

Konkle AT, McCarthy MM (2011) Developmental time course of estradiol, testosterone, and dihydrotestosterone levels in discrete regions of male and female rat brain. Endocrinology 152:223–235.

Kow LM, Pfaff DW (2004) The membrane actions of estrogens can potentiate their lordosis behavior-facilitating genomic actions. Proc Natl Acad Sci USA 101:12354–12357.

Kretz O, Fester L, Wehrenberg U, Zhou L, Brauckmann S, Zhao S, Prange-Kiel J, Naumann T, Jarry H, Frotscher M, Rune GM (2004) Hippocampal synapses depend on hippocampal estrogen synthesis. J Neurosci 24:5913–5921.

Kumar D, Boehm U (2014) Conditional genetic transsynaptic tracing in the embryonic mouse brain. J Vis Exp 94:

Kumar D, Freese M, Drexler D, Hermans-Borgmeyer I, Marquardt A, Boehm U (2014) Murine arcuate nucleus kisspeptin neurons communicate with GnRH neurons in utero. J Neurosci 34:3756–3766.

Kumar D, Periasamy V, Freese M, Voigt A, Boehm U (2015) In utero development of kisspeptin/GnRH neural circuitry in male mice. Endocrinology 156:3084–3090.

Lamprecht SA, Kohen F, Ausher J, Zor U, Lindner HR (1976) Hormonal stimulation of oestradiol-17 beta release from the rat ovary during early postnatal development. J Endocrinol 68:343–344.

Lauber ME, Lichtensteiger W (1994) Pre- and postnatal ontogeny of aromatase cytochrome P450 messenger ribonucleic acid expression in the male rat brain studied by in situ hybridization. Endocrinology 135:1661–1668.

Lehman MN, Coolen LM, Goodman RL (2010) Minireview: kisspeptin/neurokinin B/dynorphin (KNDy) cells of the arcuate nucleus: a central node in the control of gonadotropin-releasing hormone secretion. Endocrinology 151:3479–3489.

Lephart ED, Simpson ER, McPhaul MJ, Kilgore MW, Wilson JD, Ojeda SR (1992) Brain aromatase cytochrome P-450 messenger RNA levels and enzyme activity during prenatal and perinatal development in the rat. Brain Res Mol Brain Res 16:187–192.

Mayer C, Acosta-Martinez M, Dubois SL, Wolfe A, Radovick S, Boehm U, Levine JE (2010) Timing and completion of puberty in female mice depend on estrogen receptor alpha-signaling in kisspeptin neurons. Proc Natl Acad Sci USA 107:22693–22698.

McCarthy MM (2008) Estradiol and the developing brain. Physiol Rev 88:91–124.

Micevych PE, Meisel RL (2017) Integrating neural circuits controlling female sexual behavior. Front Syst Neurosci 11:42.

Mombaerts P, Wang F, Dulac C, Chao SK, Nemes A, Mendelsohn M, Edmondson J, Axel R (1996) Visualizing an olfactory sensory map. Cell 87:675–686.

Paxinos G, Halliday GM, Watson C, Koutcherov Y, Wang H (2007) Atlas of the developing mouse brain. Cambridge, MA: Elsevier.

Pielecka-Fortuna J, Chu Z, Moenter SM (2008) Kisspeptin acts directly and indirectly to increase gonadotropin-releasing hormone neuron activity and its effects are modulated by estradiol. Endocrinology 149:1979–1986.

Ruka KA, Burger LL, Moenter SM (2016) Both estrogen and androgen modify the response to activation of neurokinin-3 and kappa-opioid receptors in arcuate kisspeptin neurons from male mice. Endocrinology 157:752–763.

Sanghera MK, Simpson ER, McPhaul MJ, Kozlowski G, Conley AJ, Lephart ED (1991) Immunocytochemical distribution of aromatase cytochrome P450 in the rat brain using peptide-generated polyclonal antibodies. Endocrinology 129:2834–2844.

Santen RJ, Brodie H, Simpson ER, Siiteri PK, Brodie A (2009) History of aromatase: saga of an important biological mediator and therapeutic target. Endocr Rev 30:343–375.

Sasano H, Takashashi K, Satoh F, Nagura H, Harada N (1998) Aromatase in the human central nervous system. Clin Endocrinol (Oxf) 48:325–329.

Scarduzio M, Panichi R, Pettorossi VE, Grassi S (2013) Synaptic long-term potentiation and depression in the rat medial vestibular nuclei depend on neural activation of estrogenic and androgenic signals. PLoS One 8: e80792.

Schambra U (2008) Prenatal mouse brain atlas. New York: Springer.

Scordalakes EM, Rissman EF (2004) Aggression and arginine vasopressin immunoreactivity regulation by androgen receptor and estrogen receptor alpha. Genes Brain Behav 3:20–26.

Stanic D, Dubois S, Chua HK, Tonge B, Rinehart N, Horne MK, Boon WC (2014) Characterization of aromatase expression in the adult male and female mouse brain: I. Coexistence with oestrogen receptors alpha and beta, and androgen receptors. PLoS One 9:e90451.

Toran-Allerand CD (1976) Sex steroids and the development of the newborn mouse hypothalamus and preoptic area in vitro: implications for sexual differentiation. Brain Res 106:407–412.

Toran-Allerand CD (2005) Estrogen and the brain: beyond ER-alpha, ER-beta, and 17beta-estradiol. Ann NY Acad Sci 1052:136–144.

Toran-Allerand CD, Hashimoto K, Greenough WT, Saltarelli M (1983) Sex steroids and the development of the newborn mouse hypothalamus and preoptic area in vitro: III. Effects of estrogen on dendritic differentiation. Brain Res 283:97–101.

Travison TG, Vesper HW, Orwoll E, Wu F, Kaufman JM, Wang Y, Lapauw B, Fiers T, Matsumoto AM, Bhasin S (2017) Harmonized reference ranges for circulating testosterone levels in men of four cohort studies in the United States and Europe. J Clin Endocrinol Metab 102:1161–1173.

Unger EK, Burke KJ Jr, Yang CF, Bender KJ, Fuller PM, Shah NM (2015) Medial amygdalar aromatase neurons regulate aggression in both sexes. Cell Rep 10:453–462.

Vanacker C, Moya MR, DeFazio RA, Johnson ML, Moenter SM (2017) Long-term recordings of arcuate nucleus kisspeptin neurons reveal patterned activity that is modulated by gonadal steroids in male mice. Endocrinology 158:3553–3564.

Ventura-Aquino E, Paredes RG (2020) Sexual behavior in rodents: where do we go from here? Horm Behav 118:104678.

Vreeburg JT, van der Vaart PD, van der Schoot P (1977) Prevention of central defeminization but not masculinization in male rats by inhibition neonatally of oestrogen biosynthesis. J Endocrinol 74:375–382.

Wacker DW, Khalaj S, Jones LJ, Champion TL, Davis JE, Meddle SL, Wingfield JC (2016) Dehydroepiandrosterone heightens aggression and increases androgen receptor and aromatase mRNA expression in the brain of a male songbird. J Neuroendocrinol 28:12443.

Wagner CK, Morrell JI (1997) Neuroanatomical distribution of aromatase MRNA in the rat brain: indications of regional regulation. J Steroid Biochem Mol Biol 61:307–314.

Walker VR, Korach KS (2004) Estrogen receptor knockout mice as a model for endocrine research. ILAR J 45:455–461.

Wang L, Burger LL, Greenwald-Yarnell ML, Myers MG Jr, Moenter SM (2018) Glutamatergic transmission to hypothalamic kisspeptin neurons is differentially regulated by estradiol through estrogen receptor alpha in adult female mice. J Neurosci 38:1061–1072.

Wen S, Gotze IN, Mai O, Schauer C, Leinders-Zufall T, Boehm U (2011) Genetic identification of GnRH receptor neurons: a new model for studying neural circuits underlying reproductive physiology in the mouse brain. Endocrinology 152:1515–1526.

Wu MV, Manoli DS, Fraser EJ, Coats JK, Tollkuhn J, Honda S, Harada N, Shah NM (2009) Estrogen masculinizes neural pathways and sex-specific behaviors. Cell 139:61–72.

Yang Y, Fang Z, Dai Y, Wang Y, Liang Y, Zhong X, Wang Q, Hu Y, Zhang Z, Wu D, Xu X (2018) Bisphenol-A antagonizes the rapidly modulating effect of DHT on spinogenesis and long-term potentiation of hippocampal neurons. Chemosphere 195:567–575.

Yeo SH, Kyle V, Morris PG, Jackman S, Sinnett-Smith LC, Schacker M, Chen C, Colledge WH (2016) Visualisation of Kiss1 neurone distribution using a Kiss1-CRE transgenic mouse. J Neuroendocrinol 28:12435.

Yip SH, Boehm U, Herbison AE, Campbell RE (2015) Conditional viral tract tracing delineates the projections of the distinct kisspeptin neuron populations to gonadotropin-releasing hormone (GnRH) neurons in the mouse. Endocrinology 156:2582–2594.